Free-Energy-Driven Transfer of Charge in Dense Electrochemically Active Monomolecular Films

Dmitry Zaslavsky,[†] Andrei Pakoulev,[‡] and Vladimir Burtman*[,‡]

University of Illinois, School of Chemical Sciences, 600 South Mathews Street, Urbana, Illinois 61801

Received: June 20, 2004; In Final Form: July 26, 2004

The interest in monomolecular films as electric conductors arises from the search for innovative materials. The lateral charge transfers in noncovalently bonded films are limited to the distances in the order of a micrometer because they are mechanically unstable and consist of poorly connected domains. Here, we show that a recently developed gas-phase assembling method, which produces robust dense monolayers of NTCDI (1,4,5,8-naphthalene tetracarboxylic diimide) covalently attached to the surface of silicon, allows one to overcome this scale limitation. These virtually insulating monolayers can be photochemically populated with cation radicals via ejection of electrons into the semiconducting base. The positive charges of cation radicals can migrate as far as several millimeters within microseconds in a random walk fashion thus demonstrating the macroscopic connectivity of the film. Since the charges exist as cation radicals, which are potent oxidants, their migration is coupled to transfer of the free energy of their reduction and is driven by the redox potential gradient. Reduction of cation radicals by an anode converts this free energy into electromotive force. We show how these films can be implemented in solar energy conversion and basic time-resolved distance-controlled studies of sequences of ultrafast electron transfers.

Introduction

The fundamentals of electron transfers were revealed by analysis[1−4] of electron transfers in structurally defined natural and synthetic molecules. These studies accounted for the role of the intervening medium that couples redox centers and introduced σ-coupling (via covalent or hydrogen bonds) and π-coupling (via overlapping π-orbital) and through-space jumps and thus refined the empiric rule of the exponential drop in the tunneling rate constant as the width of the separating barrier increases.

Even though the σ-coupling is efficient within macrochains[5] or thick films,[6] the ways of creating extended continuous σ-coupled 2D networks are yet to be found. Despite that π- and through-space couplings provide smaller range for the single-barrier tunneling[7] than the σ-coupling,[8−10] the multistep electron transfer through the π-stacked purine strands of DNA has proved itself efficient.[6,9,10] Thus, in redox-active polymers[3−5] and biological electron-transfer complexes,[8,9] the exponentiality problem is overcome by switching to the multistep transport through a continuous network of σ-coupled redox centers.

The noncovalently bonded monomolecular films can provide connectivity between redox centers within grains of typically a micrometer or even smaller.[3] Extension of the network into the macroscale requires stabilization of the structure, preferably by covalent bonding, making the network rigid. At the same time, the number of defects introduced into the structure during the assembly has to be kept minimal to avoid formation of isolated domains. Therefore, the electrochemically active "building" elements have to be small to ease their packing. Advantageously, macroscopic π-stacked 2D networks of small aromatic diimides can be assembled on solid surfaces by the recently developed method[11,12] utilized in this work (Figure 1A). We show that these monomolecular films can sustain charge transfer over at least several millimeters. This long-range charge transfer originates from and testifies for the macroscopic connectivity of the fabricated films. This connectivity can be used in many applications including solar cells and photomultipliers.

Methods

Preparation of Organic Films. Thick, impermeable to light, wafers of n-type (500 Ω cm, Virginia Semiconductors) Si(100) having 20 Å of SiO_2 coating and glass slides were cleaned and functionalized with amino groups (step a) as described in ref 11. NTCDA (1,4,5,8-naphthalene tetracarboxylic anhydride) evaporated at 110 °C and reacted with the NH_2-functionalized surface for 45 min in a Bell Jarr chamber at 10^{-5} Torr (step b). The product of assembly lacks the amino group preventing formation of the second layer. The substrate was kept on a heated sample holder (180 °C) preventing physadsorption of the precursor. Vacuum deposition modified over 60% of the surface amino groups.[12] A layer of 4-aminophenylthiol was added within 20 min (step c). This reaction tops the surface with SH-groups reactive toward metals.[13] The chip was gently rinsed with 2-propanol and heated at 80 °C for 1 h. A silver contact was placed on top of the films by placing a drop of colloidal silver in acetonitrile and allowing the solvent to evaporate; the area or the contact between the silver and the coated silicone was ∼3 mm^2. Thick (∼300 nm) films of NTCDA and C6-NTCDI were prepared by physadsorption of NTCDA on the cold functionalized surface of silicon. Sparse NTCDI films were obtained from thick films of NTCDA by heat desorption of the excess of NTCDA followed by step c.

Characterization of the NTCDI Monolayer. A step-by-step buildup of the layers was characterized by contact angle (CA)

* Correspondence and requests for materials should be addressed to this author. Current address: University of Utah, Department of Physics; e-mail: burtman@physics.utah.edu.

[†] Department of Biochemistry.

[‡] Department of Chemistry.

10.1021/jp047315b CCC: $27.50
Published on Web 09/10/2004

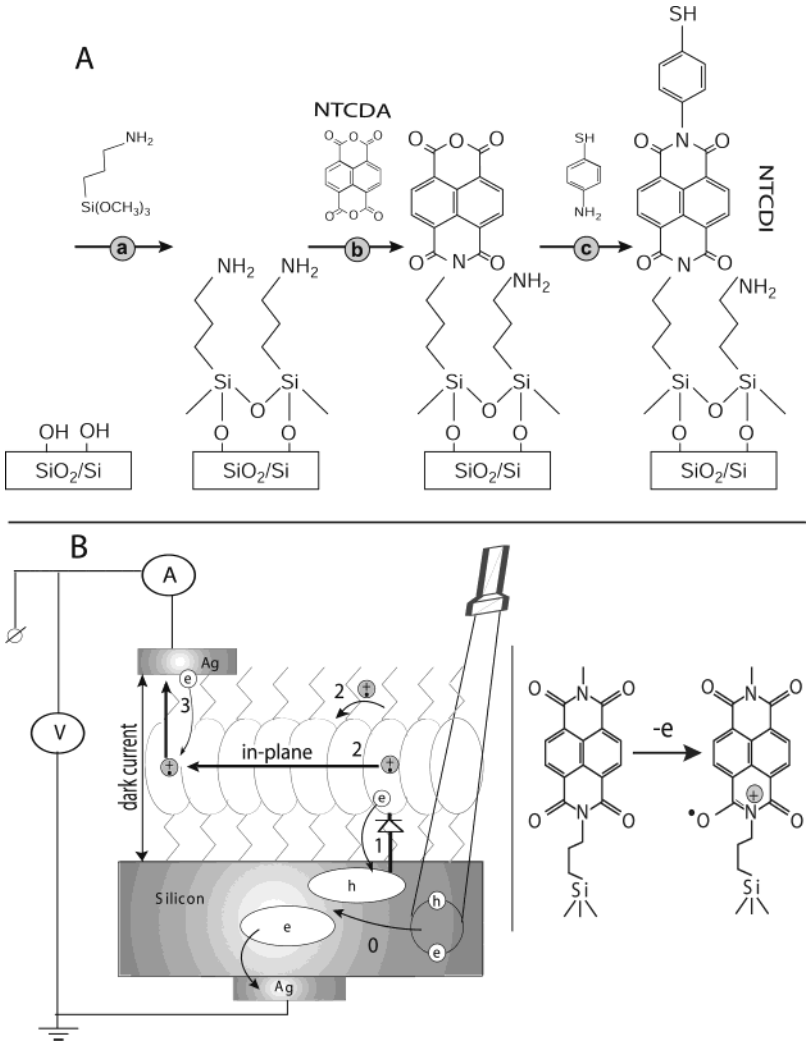

Figure 1. Fabrication and operation of the photoelement. (A) The three-step assembly of monomolecular films of NTCDI. (B) Incident light creates holes (h) in the valence band of silicon. Upon ejection of electrons (reaction 1) from the immobilized molecules into the holes, cation radicals are formed (inset). Cation radicals rapidly exchange with the neutral molecules (2); the positive charge travels through the film, resulting in the in-plain current. Rereduction of cation radicals by silver (3) completes the photovoltaic element. Reactions 1−3 generate electromotive force. The diode (1) reflects rapid photoejection of electrons from the film and slow back-reaction. The external electric connections used in the voltammetric experiments (Figure 2) include a power source, an ammeter, and a voltmeter.

changes, IR spectroscopy, XPS, and UV−vis spectroscopy.The results agree well with previous characterization[11,12] of NTCDI SAM monolayers and are briefly summarized below. After step a, CA changed from 17° to 45°, and the appearance of the 3200 cm^{-1} alkylamine IR peak was observed. The N (1s) XPS core level spectra showed a predominantly 398.8 eV (85%) peak on the amine surface because of the nonprotonated NH_2-group.[14] The minor N1(s) component at 400.6 eV is attributed to protonated NH_3^+ (15%). The UV−vis spectrum of the film grown on the glass slide did not reveal any peaks. After step b, the CA changed from 45° to 92° and the 1655 cm^{-1} IR peak of the imide bond formation was detected. In accord with previous studies,[15] formation of imides on the surface results in disappearance of the majority of the original peaks at 400.6 eV (29%) and 399.8 eV and formation of a new single broad N(1s) peak at 399.6 eV (67%) because of formation of imido groups with a possible presence of amido groups.[16] When step b was performed on a glass slide, two peaks appeared in the UV spectrum: 360 and 390 nm; OD ∼ 0.004 and 0.006, respectively (Figure 3). We also observed an appearance of a new broad peak in the greenish-orange region (OD = 0.001) that characterized a formation of an in-plane ordered organic heterostructure in SAM structure. After step c, the CA changed from 92° to 60° and a new peak (236 eV) associated with HS groups was observed in the XPS spectrum. No significant changes were found in the UV−vis and the IR spectra after step c.

Variable angle spectroscopic ellipsometery (VASE, Woollam Co.) was used to verify the monolayer growth as it was reported for NTCDI SAM structure.[11,12,17] The variable angle spectroscopic ellipsometer measured spectra with 5-nm intervals in the range 300−1700 nm. The structural model for fitting ex-situ ellipsometry data uses the data of three different incident angles: 65°, 70°, and 75°. Measured and fitted ellipsometric data for a structure containing Si/SiO2, siloxane matrix, NTCDI-benzene thiol exhibit molecular *c*-axis interplanar spacing are 20 Å for SiO_2 native oxide, 3.5 Å for the siloxane matrix, 7.0 Å for NTCDI, and 6.9 Å for the benzene thiol layer.

Determination of the Absorption and External Quantum Efficiencies. The spectra of dense and sparse monolayers of NTCDI grown on glass slides were recorded in a Shimadzu spectrophotometer. Comparison of the films grown on Si and glass is justified by the surface titration, which shows that the density of amino groups on glass and SiO_2 coating of Si(100) is approximately the same[17] (2−3 per 100 $Å^2$). The EQE was calculated as a ratio of the number of electrons passed through a 500 Ω resistor to the number of photons in the light flow.

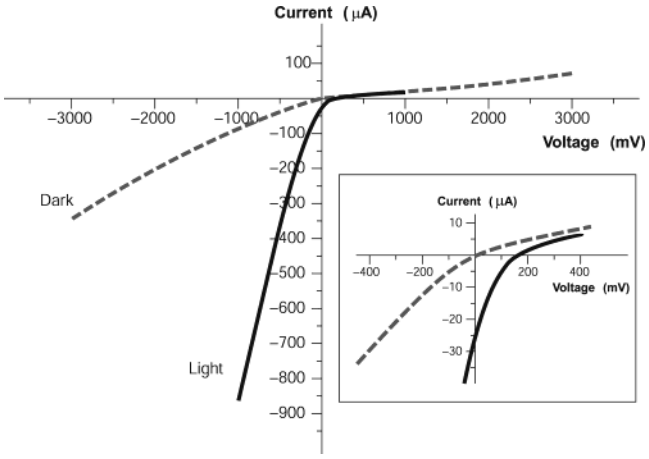

Figure 2. Electrooptical properties of the Si/NTCDI/Ag heterostructure. All experiments have been carried out at room temperature. Constant monochromatic 400-nm light illuminated an ~10-mm spot centered ~5 mm away from the silver electrode. When the Ag electrode is highly electronegative, the element behaves as a photoamplifier and light noticeably increases the asymmetry of the I−V curve.

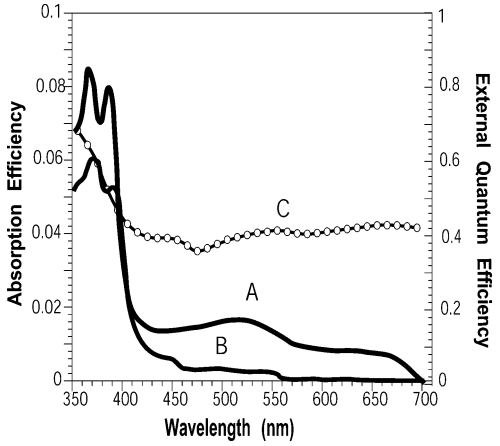

Figure 3. Effect of the surface density of NTCDI on the film spectra and light-harvesting efficiency. Dense film A assembled on glass has a prominent aggregation band in the greenish-orange region. The external quantum efficiency of the corresponding Si cell illuminated by constant nonsaturating light is represented by spectrum C. Sparse film B has no aggregation band in the spectrum. The external quantum efficiency of the corresponding cell was too low to measure.

The output of a Xenon lamp/monochromator assembly (8-nm bandwidth) standardized to the Oriel calibrated light source was used to illuminate the photoelement. The EQE was also measured at 532 nm by referring to nonsaturating output of CW YAG laser calibrated with a photocalorimeter.

Time-Resolved Photovoltage Measurements. These were performed with a picosecond laser system consisting of a Ti: Sapphire femtosecond laser, stretcher/compressor/amplifier of picosecond laser pulse ("Titan", Quantronix), and optical parametric amplifier of superflourescense ("TOPAS", Qunantronix/Light Conversion). The output pulse parameters were wavelength 532 nm, energy 10 μJ, pulse duration 1 ps, and repetition rate 1 kHz. To avoid saturation effects, the pulse energy was attenuated to a 0.1 μJ level with a beam diameter of 1 mm. The photovoltage transients were recorded by Tektronix TDS 3025 digital oscilloscope bypassed with a 7.6 kΩ resistor.

Results and Discussion

We topped the film with a small-area silver electrode and found that the resulting Ag/NTCDI monolayer/Si sandwich (Figure 1B) was sensitive to light. In the dark, the current−voltage (I−V) curve goes through the origin (Figure 2) and straightens at the slopes that correspond to ~30 and ~10 kΩ, respectively, as the positive or negative voltage increases. Illumination with continuous monochromatic light changes this characteristic dramatically. Now, the I−V curve also goes through the bottom right quadrant where the current through the element opposes the external bias. This plainly manifests that light generates electromotive force, which induces a negative charge on silicon (photocathode) and a positive charge on silver (photoanode). The maximal photovoltage at the saturating light power was as high as 280 mV. In the absence of the film or only with the amino layer present, the maximal photovoltage was below 0.1 mV and could not be characterized accurately.

The mutual arrangement of the cell and the incident light, the external quantum efficiency (EQE) of 0.4−0.7 (Figure 3), which cannot be accounted for by the absorption efficiency of the film, the dissimilarity of the EQE, and the absorption efficiency of the film and resemblance of EQE to the spectrum of silicon[19] suggest that the light is productively absorbed by the semiconductor (Figure 1B). This contrasts with light harvesting in the dye-sensitized photovoltaic cells[20,21] or the hybrid nanorod−polymer cells,[22] which require special junctions with enormous contact areas between the materials to enhance their absorption efficiency. The geometry of the cell also suggests that light harvesting incorporates a longitudinal spatial energy transfer.

In contrast to natural photosynthesis,[23] the conserved energy does not migrate in the form of excitation. The absence of long-range light harvesting, when the uncoated side of the chip was illuminated, establishes importance of the film and rules out energy transfer within the silicon bulk. The process starts with a redox reaction separating charges between silicon and film (reaction 1). Because of the spatial separation of the cathode and the anode chemistry, this reaction can be identified straight from the polarity of the cell, which shows that electrons from the NTCDI molecules are ejected into silicon, that is, NTCDI molecules oxidize. Charge separation is supported by the asymmetry of multiplication of the dark current with respect to the bias direction (Figure 2), which cannot be accounted for by the influence of nonpolar excited states. Indeed, regardless of the amplification mechanism, they would not be able to discriminate the bias directions. On the contrary, charge separation explains this asymmetry easily. Since the positive charges in the NTCDI film "reflect" in silicon "mirror", they are accompanied by their countercharged electrostatic images and migrate as trans-surface dipoles. As these dipoles approach the Ag/film/Si junction, they are either attracted into the contact area by parallel or repelled by the antiparallel external field. In agreement with photooxidation mechanism of energy conservation, light harvesting was observed in the thick films of *N*,*N*′-dihexyl-naphthalene tetracarboxylic diimide (C_6-NTCDI) physadsorbed on the silicon surface, but not in the thick films of NTCDA, because NTCDA is much harder to oxidize.

This photooxidation incorporates several events. Absorption of light results in elevation of an electron to the conductance band leaving a vacancy in the valence band. This vacancy can be filled either by back recombination of the electron from the conductance band (unproductive decay) or by transfer of an electron from the film into silicon (reaction 1) since the affinity of this vacancy for an electron is apparently high enough to oxidize a molecule of NTCDI. As a result, similarly to the photochemistry of dye-sensitized cells,[21,22] an extra electron remains in the conductance band of silicon, while the oxidized

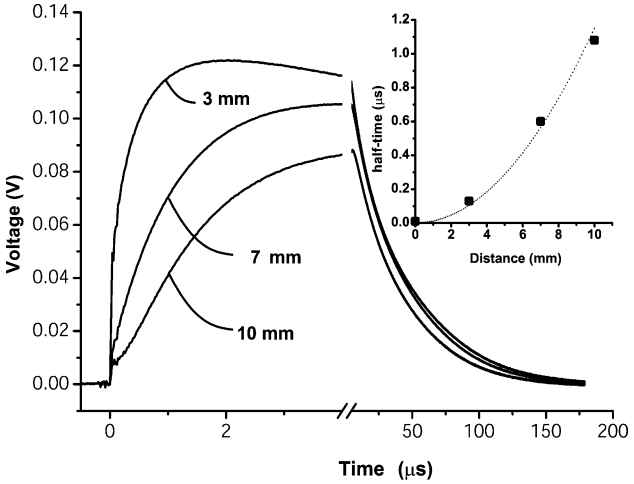

Figure 4. Scanning time-resolved photovoltage probing. The transients were induced by pulses centered at different distances apart from the silver electrode. The inset shows the dependency of the $T_{1/2}$ of the voltage rise on the distance l between the bright spot and the silver photoanode. The solid line approximates the points by a parabola $T_{1/2} = l^2/D$ with the parameter $D \sim 10^6$ cm^2/s.

molecules of NTCDI become cation radicals (Figure 1B, inset). These radicals resemble those in protein[24,25] and DNA[26] molecules and combine essential structural motifs of the oxidized forms of two ubiquitous redox cofactors: NAD^+ and semiquinone. These features ease oxidation of neutral molecules.

The energy of light is conserved in two forms: the electrostatic energy of trans-surface dipoles and the free energy of reduction of cation radicals by silver (reaction 3). The equilibrium of this reaction is shifted toward neutralization of cation radicals, and we could not attain electric currents in the films assembled on the surface of glass because measurements of such currents even over microgaps require very sensitive equipment.[27] To study migration of cation radicals to the photoanode (reaction 2), we used short light pulses focused at different distances from the anode to provide both time and spatial resolution. The photovoltage transients consist of voltage rise and decay (Figure 4). The decay is exponential with $\tau \sim 40$ μs at the given external load. This component represents the discharge of the cell because of both the backflow and the functional current through the load.

The voltage rise originates from accumulation of charges at the anode and its kinetics depends on the distance between the illuminated spot and silver (Figure 4). To avoid a model bias, we described the kinetics of the voltage rise by its half-time $T_{1/2}$ (Figure 4, inset), which reflects the travel time of the cation radicals. Despite some spatial uncertainty due to the finite beam size and a limited number of data points, one can see that the travel time appears to be proportional to the second power of the distance between the illuminated area and the silver electrode rather than to its first power. Since the area (distance quadrate) covered by a random-walking particle is proportional to its travel time, this dependency (Figure 1B, reaction 2) is consistent with the random walk fashion of migration of cation radicals within the film during successive self-exchange reactions between the neutral molecules and the cation radicals. It is driven by the spatial gradients of their electrochemical potential, which are present because the anode reduces the cation radicals. Migration of cation radicals requires proximity of the molecules forming the monolayer and acting as redox centers. Such proximity manifests itself as a broad absorbance band in the green-orange region (Figure 3), attributed (ref 11) to formation of closed packed aggregate channel. This migration, that is, time-resolved growth of the photovoltage, was not observed in the sparse monolayers of NTCDI, in the thick films of NTCDA, or without organic film. Only minor signals were observed in these control devices especially with the laser beam incident at the edge of the Ag contact. When the center of the beam was moved away from the edge, these signals disappeared rather than develop slower.

The slight decrease of the total charge collected by the anode is probably due to partial recombination of trans-surface dipoles. However, the lifetime of cation radicals is apparently somewhat longer than the travel times of ~ 1 μs or less at the given distances. The similar back recombination in the dye-sensitized TiO_2 takes milliseconds.[28]

The charges formed in the remote-illuminated area have to travel within the film over "gigantic" distances at finite speed. Therefore, the beginning of the voltage rise should lag behind the initial rapid charge separation. The small initial signal (Figure 4), which was also present in the sparse films and was especially strong when the edge of the Ag anode was illuminated, allowed only qualitative studies of this delay. However, when the beam was focused 10 mm away from the anode, a $\sim$100-ns lag became visible, providing a rough estimate for the velocity of migrating charges about $\sim 10^5$ m/s ($\sim$1 fs/Å). This lag has never been observed in the molecules of DNA where cation radicals can migrate over $\sim$100$-$200 Å, depending on the composition of these molecules.[6,13,15] Under most experimental conditions, the overall transfer over these distances is limited by the radical formation[29] hiding the related lag, expected to be about $\sim$100 fs.

The vast majority of studies of lateral charge transfer in monomolecular structures were limited to the self-assembling and Langmuir$-$Blodgett monolayers.[30$-$32] Some of these studies have revealed that electrochemical activity of the assembling molecules is a requirement for charge transfer within these monolayers.[33,34] In analogy to that we believe that the efficient delivery of positive charges to the photoanode becomes possible because of the macroscopic connectivity of the network of NTCDI molecules acting as redox centers. This connectivity permits rapid transfer of large net charge through an extremely narrow cross section and originates from assembling NTCDI molecules at the positions predetermined by arrangement of the NH_2-groups within the dense interlinked siloxane network.[35] These networks, stabilized by bonding to solid surface, can be used for coupling electrodes in detectors or organic solar cells, which will utilize semiconductors with high absorption efficiency as the light-harvesting antennas. Their configuration is reverse to that of the dye-sensitized cells[21,22] and their components act as photooxidant, charge-energy relay and fuel.

Acknowledgment. We thank Prof. A. Gewirth, Prof. R. Gennis for their generous support of this work, Prof. D. Dlott, Dr. R. Hash, and Dr. R. Strange for the use of their instrumentation. Writing of the manuscript was greatly facilitated by discussions with Prof A. Gewirth, Prof. R. Gennis, Prof. H. B. Gray, Dr. A. Yakimov, and Dr. D. Rykunov. We thank E. Kiselov for graphic design and Dr. P. Tsatsos for proofreading the manuscript.

References and Notes

(1) Markus, R. A.; Sutin, N. *Biochim. Biophys. Acta* **1985**, *811*, 265.
(2) Moser, C. C.; Keske, J. M.; Warncke, K.; Farid, R. S.; Dutton, P. L. *Nature* **1992**, *355*, 796.
(3) Winkler, J. R.; Di Bilio, A. J.; Farrow, N. A.; Richards, J. H.; Gray, H. B. *Pure Appl. Chem.* **1999**, *71*, 1753.
(4) Onuchik, J. N.; Beratan, D. N.; Winkler, J. R.; Gray H. B. *Annu. Rev. Biophys. Biomol. Struct.* **1992**, *21*, 349.

(5) Georgiadis, R.; Peterlinz, K. A.; Rahn, J. R.; Peterson, A. W.; Grassi, J. H. *Langmuir* **2000**, *16*, 6759.
(6) Wamser C. C.; Bard, R. R.; Senthilathipan, V.; Anderson, V. C.; Yates, J. A.; Lonsdale, H. K.; Rayfield, G. W.; Friesen, D. T.; Lorenz, D. A.; Stangle, G. C.; van Eikeren, P.; Baer, D. R.; Ransdell, R. A.; Golbeck, J. H.; Babcock, W. C.; Sandberg, J. J.; Clarkel, S. E. *J. Am. Chem. Soc.* **1989**, *111*, 8485.
(7) Liu, C.-S.; Schuster, G. B. *J. Am. Chem. Soc.* **2003**, *125*, 6098.
(8) Porath, D.; Bezryadin, A.; de Vries, S.; Dekker, C. *Nature* **2000**, *403*, 635.
(9) Porath, D.; Bezryadin, A.; de Vries, S.; Dekker, C. *Nature* **2000**, *403*, 635.
(10) Berlin, Y. A.; Burin, A. L.; Ratner, M. A. *J. Am. Chem. Soc.* **2001**, *123*, 260.
(11) Burtman, V.; Zelichenok, A.; Yitzchaik, S. *Angew. Chem., Int. Ed.* **1999**, *38*, 2041.
(12) Burtman, V.; Offir, Y.; Yitzhaik, S. *Langmuir* **2000**, *17*, 2137.
(13) Whitesides, G. M.; Laibinis, P. E. *Langmuir* **1990**, *6*, 87.
(14) Ada, E. T.; Hanley, L.; Etchin, S.; Melngailis, J.; Dressick, W. J.; Chen, M.-S.; Calvert, J. M. *J. Vac. Sci. Technol., B* **1995**, *13*, 2189.
(15) *Practical Surface Analysis*; Briggs, D., Seah, M. P., Eds.; Wiley: New York, 1990; p 444.
(16) Kallury, K. M. R.; Macdonald, P. M.; Thompson, M. *Langmuir* **1994**, *10*, 492.
(17) Burtman, V.; Zelichenok, A.; Yitzchaik, S. *Polym. Prepr.* **1998**, *39*, 167.
(18) Reference deleted in proof.
(19) Sze, S. *Semiconductor Devices Physics and Technology*; Wiley: New York, 1985.
(20) Hagfeldt, A.; Grätzel, M. *Acc. Chem. Res.* **2000**, *33*, 269.
(21) Grätzel, M. *Nature* **2001**, *414*, 338.
(22) Huynh, W. U.; Dittmer, J. J.; Alivisatos, A. P. *Science* **2002**, *295*, 2425.
(23) Glazer, A. N. *Annu. Rev. Biochem.* **1983**, *52*, 125.
(24) Di Bilio, A. J.; Crane, B. R.; Wehbi, W. A.; Kiser, C. N.; Abu-Omar, M. M.; Carlos, R. M.; Richards, J. H.; Winkler, J. R.; Gray H. B. *J. Am. Chem. Soc.* **2001**, *123*, 3181.
(25) Barry, B. A.; El-Deeb, M. K.; Sandusky P. O.; Babcock, G. T. *J. Biol. Chem.* **1990**, *265*, 20139.
(26) Kasai, H.; Yamaizumi, Z.; Berger, M.; Cadet J. *J. Am. Chem. Soc.* **1992**, *114*, 9692.
(27) Collet, J.; Lenfant, S.; Vuillaume, D.; Bouloussa, O.; Rondelez, F.; Gay, J. M.; Kham K.; Chevrot C. *Appl. Phys. Lett.* **2000**, *76*, 1339.
(28) Rehm, J. M.; McLendon, G. L.; Nagasawa, Y.; Yoshihara, K.; Moser, J.; Gra1tzel, M. *J. Phys. Chem.* **1996**, *100*, 9577.
(29) Wan, C.; Fiebig, T.; Schiemann, O.; Barton, J. K.; Zewail, A. H. *Proc. Natl. Acad. Sci. U.S.A.* **2000**, *97*, 14052.
(30) Bryce, M R.; Petty M. C. *Nature (London)* **1995**, *374*, 771.
(31) Bjørnholm, T.; Hassenkam, T.; Reitzel, N. *J. Mater. Chem.* **1999**, *9*, 1975.
(32) *Advances in Synthetic Metals Twenty Years of Progress in Science and Technology*; Bernier, P., Lefrant, S., Bidan, G., Eds.; Elsevier Science: 1999.
(33) Novák, P.; Müller, K.; Santhanam, K. S. V.; Haas, O. *Chem. Rev.* **1997**, *97*, 207.
(34) Heath, J. R.; Ratner, M. A. *Phys. Today* **2003**, *56*, 43.
(35) Ulman, A. *Chem. Rev.* **1996**, *96*, 1533.